Talanta 85 (2011) 2194–2201

Contents lists available at ScienceDirect

Talanta

journal homepage: www.elsevier.com/locate/talanta

A fluorescent "turn-on" probe for the dual-channel detection of Hg(II) and Mg(II) and its application of imaging in living cells

Yan Zhao[a], Baozhan Zheng[a], Juan Du[a,*], Dan Xiao[a,b,**], Li Yang[a]

[a] College of Chemistry, Sichuan University, Chengdu 610064, PR China
[b] College of Chemical Engineering, Sichuan University, Chengdu 610065, PR China

ARTICLE INFO

Article history:
Received 29 April 2011
Received in revised form 16 July 2011
Accepted 20 July 2011
Available online 27 July 2011

Keywords:
Dual-channel
Fluorescent
Probe
Imaging

ABSTRACT

A novel rhodamine-based fluorescent chemosensor (RND) was synthesized that contains two independent fluorophores and acts as a very sensitive, selective and reversible off–on probe for Hg(II). Importantly, this newly developed sensing system exhibited different fluorescent responses toward Hg(II) and Mg(II) at 589 nm and 523 nm, respectively. RND also displayed detectable color change upon treatment with Hg(II). Results from confocal laser scanning microscopy experiments demonstrated that this chemosensor is cell permeable and can be used as a fluorescent probe for monitoring Hg(II) or Mg(II) in living cells. This probe can also indirectly detect glutathione (GSH) and cysteine (Cys) with good linear relationships.

1. Introduction

Mercury is a major environmental and health concern as a result of its toxicity in living systems [1,2], and considerable efforts have been devoted to its detection. Despite a reduction in its industrial use as a result of stricter regulations, high concentrations of mercury are still present in many environmental areas. Therefore, the effective and selective detection of mercury is of great significance for biochemistry, environmental science and medicine [3,4]. Of the many modes of detection available, fluorescence-based methods have attracted much attention because of their simplicity, selectivity, high sensitivity, adaptability and online imaging capabilities [5–7]. Hg(II) is a heavy metal ion that is recognized as a fluorescence quencher due to the enhancement of spin–orbit coupling commonly associated with the heavy atom effect [8,9]. To date, many reported fluorescence chemosensors based on the complexation-induced fluorescence quenching mechanism [10–12] have led to the nonspecific identification of Hg(II) against a background of competing metal ions and a lower detection limit compared to the fluorescence enhancing mechanism. Therefore, it would be advantageous to design fluorescence sensors that can turn on and provide a specific response following Hg(II) recognition [13–15]. Another cation, Mg(II), is the most abundant divalent cation in cells, and it plays a critical role as an enzyme cofactor in DNA synthesis [16,17] and protein phosphorylation [18]. Recent findings confirmed that Mg(II) is a crucial modulator of cell function and that knockdown of genes encoding for magnesium transporters leads to cell death [19,20]. Mg(II) has long been regarded as a chronic regulator of cell function, but the development of Mg(II)-specific probes has not attracted much attention. However, the development of fluorescence imaging techniques can also be considered for use in Mg(II) research.

Biothiols, such as glutathione (GSH), homocysteine (Hcy), and cysteine (Cys), are critical physiological components and are extensively present in animal tissues and fluids [21,22]. They play extremely significant roles in metabolism and homeostasis. Thus, the rapid, sensitive and selective detection of biothiols is of considerable importance and interest.

Because of the outstanding spectroscopic properties [23] and binding-promoted fluorescence-enhancing process of rhodamine-based dyes [24–26], a new rhodamine derivative (RND) (as shown in Scheme 1) was designed and synthesized as a fluorescent turn-on probe for Hg(II) in two steps. The original purpose of introducing 2-hydroxy-1-naphthaldehyde into rhodamine B was to provide a suitable binding site, therefore improving the ability of complexation. Based on experimental results, it was reasonably hypothesized that the 2-hydroxy-1-naphthaldehyde group itself might also act as a Mg(II) detector through a fluorescent "turn-on" mechanism.

Rhodamine-based chemosensors have been widely used for detecting intracellular analytes [27,28]; therefore, we speculated that RND may be applicable for imaging Hg(II) in living cells. However, the strong thiophilic nature of Hg(II) [29–31] may cause

* Corresponding author. Tel.: +86 028 85415029; fax: +86 028 85416029.
** Corresponding author at: College of Chemistry, Sichuan University, Chengdu 610064, PR China. Tel.: +86 028 85415029; fax: +86 028 85416029.
E-mail addresses: lxdj@vip.sina.com (J. Du), xiaodan@scu.edu.cn (D. Xiao).

0039-9140/$ – see front matter © 2011 Elsevier B.V. All rights reserved.
doi:10.1016/j.talanta.2011.07.070

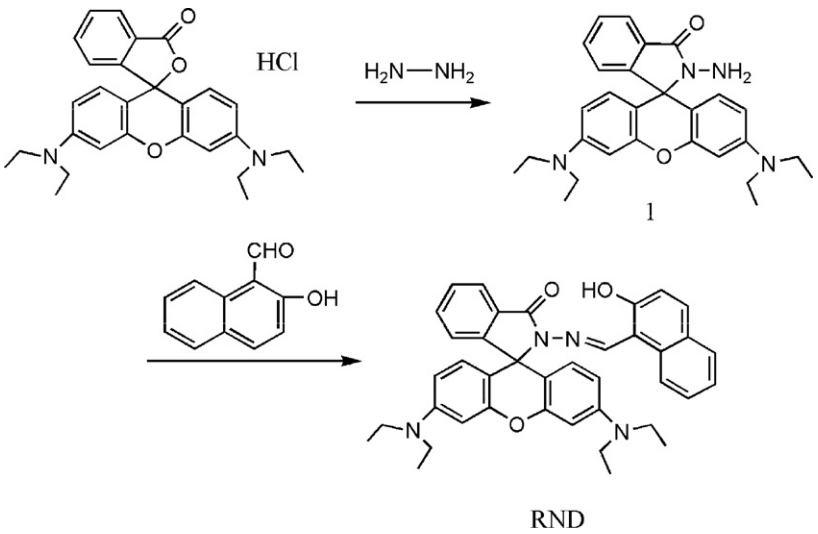

Scheme 1. Synthesis of RND.

formation of Hg–S bonds in the presence of biothiols, such as GSH and Cys. As a result, the fluorescence of RND–Hg(II) could be quenched following the addition of biothiols. Thus, the double detection of Hg(II) and biothiols based on the same fluorescent probe could be realized.

A modified previously reported procedure [32,33] was employed for the synthesis of RND. RND was synthesized from the reaction of rhodamine B and hydrazine, followed by reaction with 2-hydroxy-1-naphthaldehyde for a relatively high yield. The detailed experimental procedures are described in Section 2. The product was dissolved in 1:1 H_2O/CH_3CN (v/v), and the structure of the RND was characterized by ^{1}H NMR and MALDI-TOF MS (Figs. S1 and S2).

2. Experimental

2.1. Apparatus

^{1}H NMR measurements were performed with a Bruker AV II-600 MHz spectrometer. Fluorescence spectra were measured on a Hitachi F-4500 spectrophotometer equipped with a 1 cm quartz cell. UV–visible spectra were acquired on a Techcomp UV1100 spectrophotometer (Shanghai, China). Mass spectra were obtained with a Bruker Autoflex MALDI-TOF MS at Hong Kong Baptist University.

2.2. Chemicals

Rhodamine B was purchased from Beijing Chemical Co. Glutathione (GSH) and L-cysteine (Cys) were purchased from Aldrich Chemical Co. Hydrazine hydrate and 2-hydroxy-1-naphthaldehyde were purchased from Alfa Aesar. All solvents used for synthesis and measurements were redistilled before use. All other chemicals were of analytical-reagent grade and were used without further purification.

2.3. Cell cultures and cell labeling

Hela cells were provided by the School of Life Science at Sichuan University (Sichuan, China). Confocal fluorescence imaging was performed with a Leica TCS SP5 laser scanning confocal microscope (excitation wavelengths 543 and 403 nm). Before the experiments, the Hela cells were exposed to 100 μmol L^{-1} RND for 30 min at room temperature to allow the probe to permeate into the cells. The cells were then centrifuged to remove excess sensor, and the treated cells were then incubated with 100 μmol L^{-1} $Hg(NO_3)_2$ or 100 μmol L^{-1} $Mg(NO_3)_2$ for another 30 min. Following incubation, the cells were imaged.

2.4. Synthesis of intermediates and probes

2.4.1. Synthesis of compound *1*

For compound **1**, 2.0 mL of 98% hydrazine hydrate was added drop wise to 30 mL of vigorously stirred 2.5 mmol L^{-1} rhodamine B in ethanol at room temperature. The solution was then refluxed for 3 h. The reaction mixture was subsequently cooled, and the solvent was removed under reduced pressure with a rotary evaporator. Next, 1 mol L^{-1} HCl was added until the solution became clear. Then, 1 mol L^{-1} NaOH was slowly added with stirring until the solution pH reached 9–10. The precipitate was filtered, washed with water and dried under reduced pressure to afford compound **1** (0.83 g, yield: 70%) as a light pink powder.

2.4.2. Synthesis of RND

Compound **1** (0.46 g) was dissolved in absolute ethanol to a concentration of 1 mmol L^{-1}. An excess of 2-hydroxy-1-naphthaldehyde (0.26 g, 1.5 mmol L^{-1}) was then added, Next, the mixture was refluxed for approximately 8 h, and TLC demonstrated that the reaction was complete. The solution was then concentrated and allowed to stand at room temperature overnight. The precipitate was filtered the following day, washed several times with cold ethanol, recrystallized from absolute ethanol and dried under reduced pressure to afford RND (0.55 g, yield: 90%) as a light yellow solid.

Using ^{1}H NMR (600 MHz, D_6-DMSO, ppm), the following chemical shifts were recorded: δ 1.05(12H, t), 3.30(8H, q), 6.37(2H, dd), 6.49(4H, d), 7.10(1H, d), 7.18(1H, d), 7.35(1H, t), 7.46(1H, t), 7.62(1H, t), 7.66(1H, t), 7.84(3H, m), 7.97(1H, d), 9.53(1H, s), and 11.92(1H, s). MALDI-TOF mass spectrometry showed a peak with m/z 611.3 ($M+H^+$).

3. Results and discussion

To examine the binding properties of RND with metal ions, the colorimetric and fluorescent responses of RND to various metal ions of interest, including Mg(II), Ba(II), Cd(II), Hg(II), Pb(II), Zn(II), Ni(II), Mn(II) and Cu(II), were investigated.

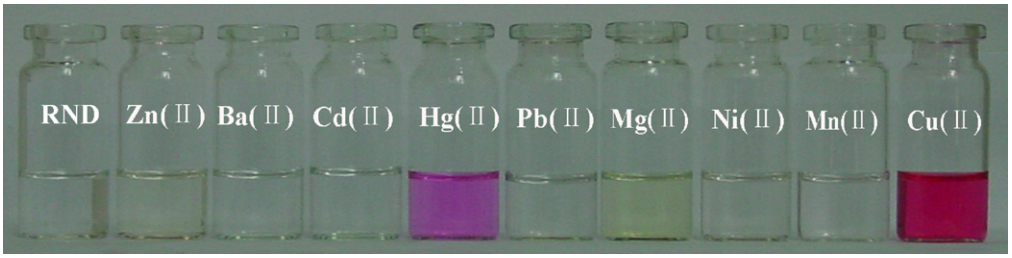

Fig. 1. Photographs of color changes of 10 μmol L^{-1} RND after the addition of 100 μmol L^{-1} various metal ions (from left to right: RND only, Zn(II), Ba(II), Cd(II), Hg(II), Pb(II), Mg(II), Ni(II), Mn(II) and Cu(II)). (For interpretation of the references to color in this figure legend, the reader is referred to the web version of this article.)

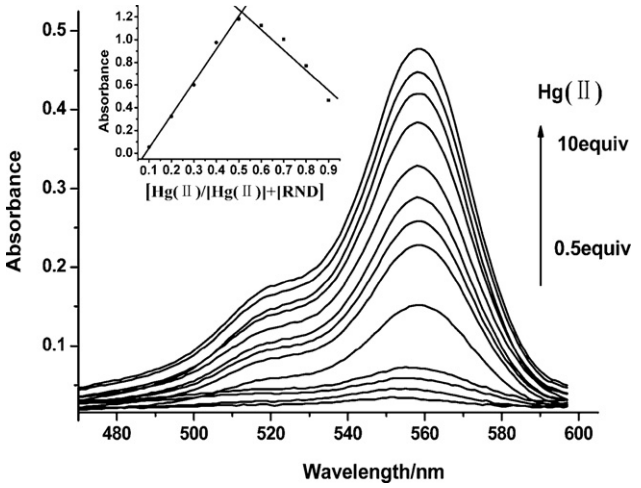

Fig. 2. Changes in absorption spectra of 10 μmol L^{-1} RND measured in acetonitrile after the addition of different amounts of Hg(II) (0.5–10 equiv.). Inset: job plot of Hg(II) versus RND ([Hg(II)] + [RND] = 100 μmol L^{-1}).

Among these metal ions, only Hg(II) and Cu(II) caused visible detectable color changes of RND solutions, i.e., from pale-yellow to magenta and red, respectively. Other metal ions did not cause any significant changes under identical conditions, as shown in Fig. 1.

Fig. 2 displays the change in the absorption spectrum of RND upon Hg(II) addition. The free RND exhibited almost no absorption peak in the visible wavelength range because of its spirolactam form. Upon addition of Hg(II), however, a new band centered at approximately 558 nm emerged, and its intensity increased gradually with increasing Hg(II) concentrations. This increase in absorbance clearly validated that RND can serve as a highly sensitive sensor for Hg(II), with color change detectable with the naked eye. Job plot (insets of Fig. 2) indicated that RND coordinated to Hg(II) in a 1:1 binding stoichiometry. Complex formation between RND and Hg(II) was also confirmed by ^{1}H NMR spectra analysis, as shown in Fig. S1. Compared to Fig. S1, Fig. S3 shows another set of signals for the RND–Hg(II) complex in addition to the set of signals for free RND. Addition of Hg(II) triggered obvious downfield proton shifts of naphthyl and aromatic moieties, which suggested that the carbonyl O, imino N and hydroxyl O atom may be involved in Hg(II) coordination. Guo et al. [34] have reported a similar observation in a NBD-TPEA-based Zn^{2+} sensor.

The fluorescent changes of RND after addition of Hg(II) were also examined in 100% CH_3CN and 1:1 CH_3CN/H_2O (v/v). Because of the solvent effect [35], it can be seen in Fig. S4 that the degree of the enhancement was different for these two solvent systems. In other words, the sensitivity of RND toward Hg(II) was much higher (~16-fold) in 100% CH_3CN than that in 1:1 CH_3CN–H_2O (v/v). To obtain optimal spectral response with this chemosensor, most of the following experiments were performed in 100% CH_3CN except for imaging Hg(II) in living cell.

Using hand-held UV light irradiation, RND alone exhibited almost no fluorescence, indicating that the predominant species of RND was the ring-closed form (Fig. 3) [36,37]. The addition of Hg(II) resulted in a prominent enhancement of fluorescence. We also found another very interesting and significant phenomenon. In addition to Hg(II), Mg(II) also induced an obvious green fluorescent response that was significantly different from the orange fluorescence caused by Hg(II).

Fig. 4 displays the fluorescence spectra of RND exposed to CH_3CN containing identical concentrations of Hg(II) and Mg(II), which were recorded using an excitation wavelength of 360 nm and emission wavelengths ranging from 450 to 650 nm. Excitation of RND at 360 nm resulted in an emission profile at 589 nm in the presence of Hg(II) and 523 nm in the presence of Mg(II). These two independent emissions of RND were well resolved, which indicated that RND could be used as a dual-tunnel fluorescent probe for Hg(II) and Mg(II) with high resolution.

In Fig. 5a, 500 nm was chosen as an excitation wavelength to obtain stronger emission intensity in the presence of Hg(II). At an emission wavelength of 589 nm, only Hg(II) induced a prominent fluorescent enhancement, which was due to the conversion of the spirolactam form to the ring-opening form of rhodamine-based dyes. The emission quantum yield (Φ) of RND with 5 equiv. of Hg(II) was evaluated to be 0.1 relative to rhodamine B (Φ = 0.97). In Fig. 5b, 360 nm was the excitation wavelength. At this wavelength, Mg(II) was the only metal ion to cause apparent fluorescent enhancement at an emission wavelength of 523 nm. Because of the different

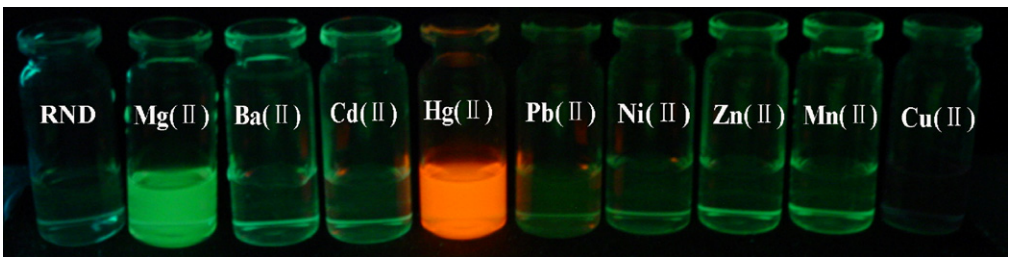

Fig. 3. Photographs of the fluorescence response of 10 μmol L^{-1} RND after the addition of 100 μmol L^{-1} various metal ions (from left to right: RND only, Mg(II), Ba(II), Cd(II), Hg(II), Pb(II), Ni(II), Zn(II), Mn(II) and Cu(II)).

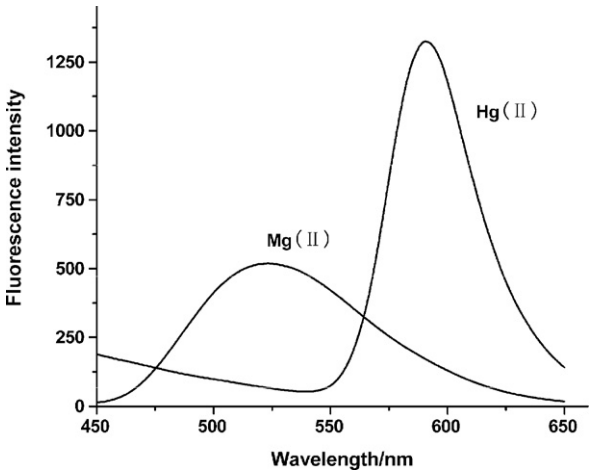

Fig. 4. Changes in the fluorescence spectra of 10 μmol L^{-1} RND measured in acetonitrile after the addition of Hg(II) and Mg(II) (10 equiv.). The excitation wavelength was 360 nm.

fluorescence behaviors above, we proposed that the binding site of RND for Mg(II) may be different from that for Hg(II). That is, Mg(II) was likely bound to the O atom of the 2-hydroxy-1-naphthaldehyde group and the N atom of the Schiff base (Fig. 6). As a result, the spirolactam form of rhodamine B would not be broken, and consequently the typical orange fluorescence of rhodamine-based dyes would not be detected. Thus, the 2-hydroxy-1-naphthaldehyde fluorophore may have played a major role in the fluorescent-on process of RND upon addition of Mg(II). A study of related mechanisms is currently being conducted by our group.

Most of the metal ions mentioned above, except for Hg(II) and Mg(II), did not show any significant fluorescence enhancement at 589 nm or 523 nm, even upon addition of 10 mol equiv. of respective metal ions.

Additionally, competition experiments (Fig. 7) demonstrated that RND maintained excellent Hg(II)-specificity in the presence of other selected metal ions.

Variation of the RND fluorescence spectra as a function of Hg(II) concentration was measured to evaluate its sensing behavior, as shown in Fig. 8a. As expected, an emission band at approximately 589 nm was observed upon addition of Hg(II). The fluorescence intensity increased with increasing Hg(II) concentrations, demonstrating the formation of a ring-opened amide form of RND. In

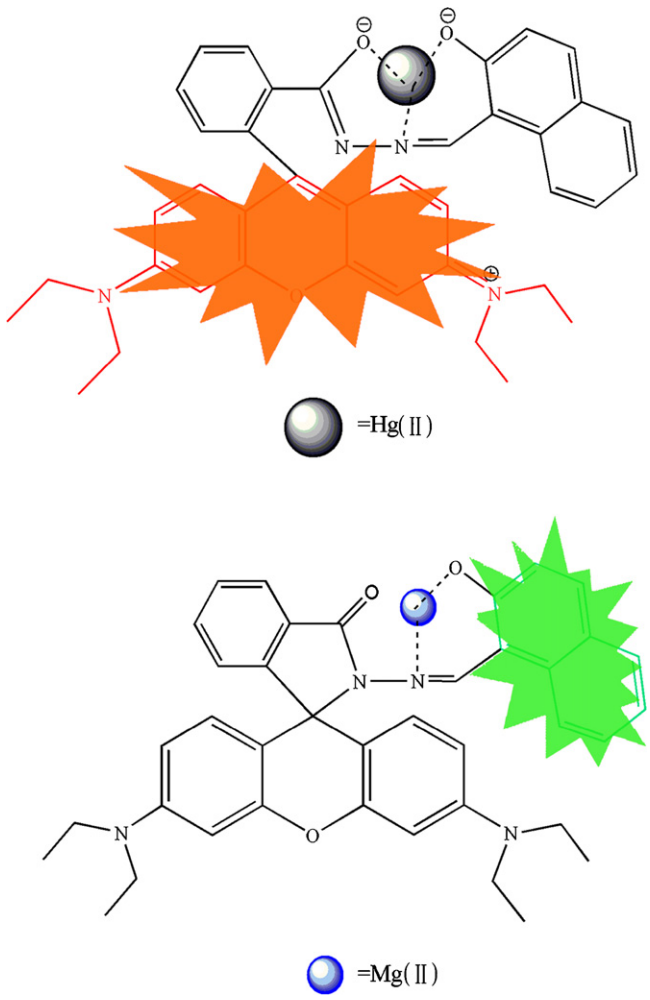

Fig. 6. Proposed binding modes of RND with Hg(II) and Mg(II).

Fig. 8a inset, The sensor exhibits a linear response toward Hg(II) at the concentration range from 0 to 25 μmol L^{-1}, the linear equation is $y = 11.2x - 12.1$ and the linear relative coefficient is $R^2 = 0.987$; from 25 μmol L^{-1} to100 μmol L^{-1}, the linear equation is $y = 1017x - 2413$ and the linear relative coefficient is $R^2 = 0.9965$,

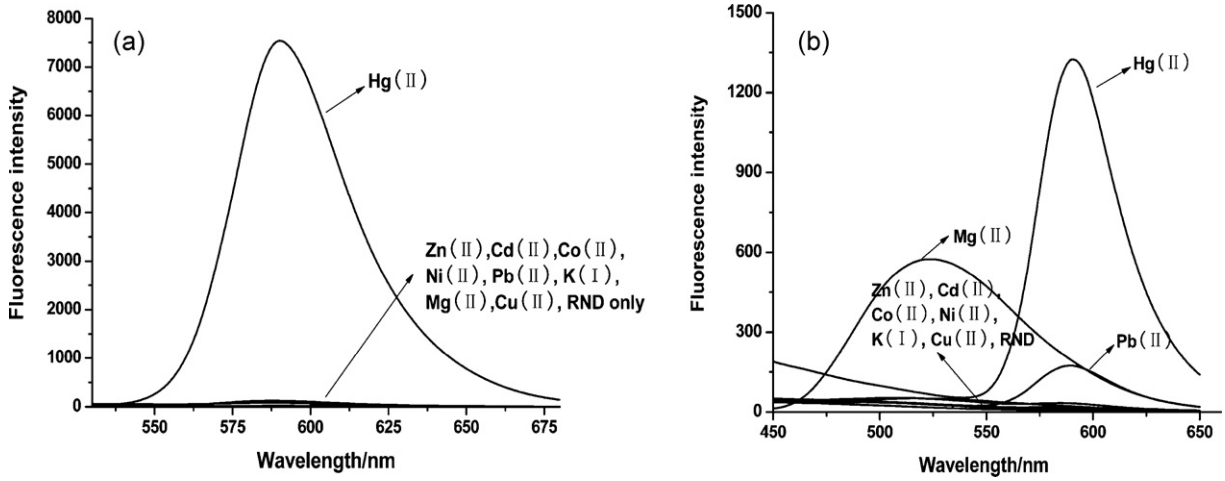

Fig. 5. (a) Changes in the fluorescence intensities of 10 μmol L^{-1} RND after the addition of different metal cations of interest (10 equiv.). The excitation wavelength was 500 nm. (b) Changes in the fluorescence intensities of 10 μmol L^{-1} RND after the addition of different metal cations of interest (10 equiv.). The excitation wavelength was 360 nm.

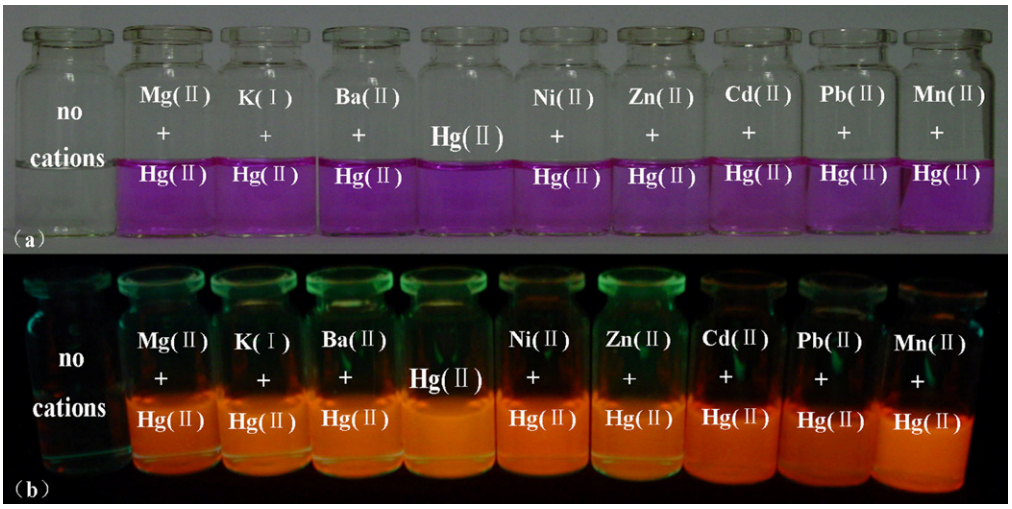

Fig. 7. (a) Photographs of the color changes after the subsequent addition of 50 μmol L^{-1} Hg(II) to a solution containing 10 μmol L^{-1} RND and 100 μmol L^{-1} cations of interest (from left to right: RND only, Mg(II), K(II), Ba(II), Hg(II), Ni(II), Zn(II), Cd(II), Pb(II) and Mn(II)). (b) Photographs of the fluorescence responses after the subsequent addition of 50 μmol L^{-1} Hg(II) to a solution containing 10 μmol L^{-1} RND and 100 μmol L^{-1} cations of interest (from left to right: RND only, Mg(II), K(II), Ba(II), Hg(II), Ni(II), Zn(II), Cd(II), Pb(II) and Mn(II)). (For interpretation of the references to color in this figure legend, the reader is referred to the web version of this article.)

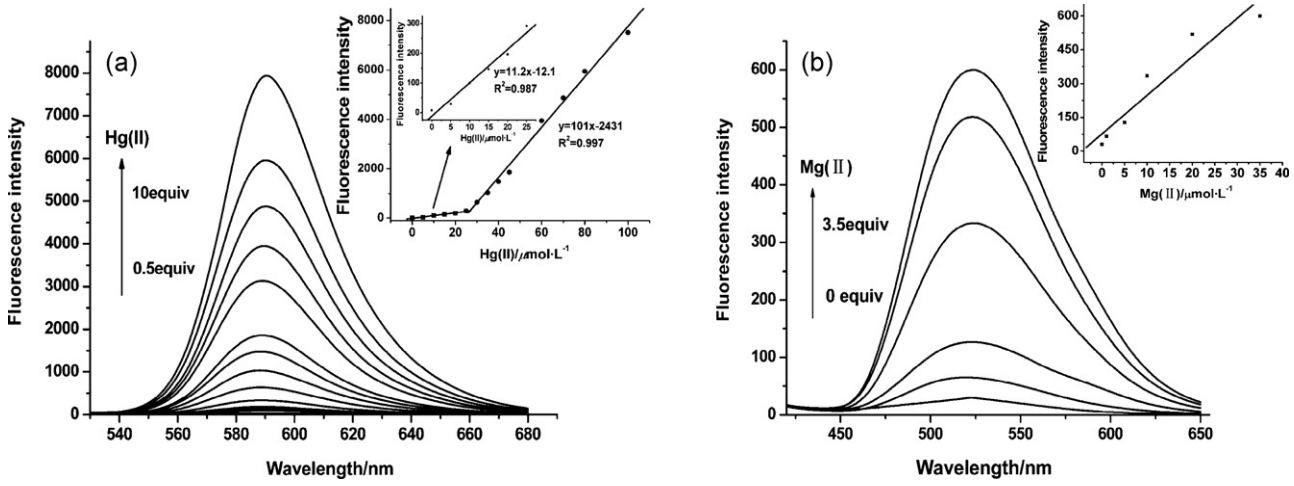

Fig. 8. (a) The changes in the fluorescence spectra of 10 μmol L^{-1} RND measured in acetonitrile after the addition of different amounts of Hg(II) (0.5–10 equiv.). The excitation wavelength was 500 nm. Inset: changes in the fluorescence intensity at 589 nm. (b) The changes in the fluorescence spectra of 10 μmol L^{-1} RND measured in acetonitrile after the addition of different amounts of Mg(II) (0–3.5 equiv.). The excitation wavelength was 360 nm. Inset: changes in the fluorescence intensity at 523 nm.

The detection limit for the sensor is estimated to be 80 nmol L^{-1} (3σ). The association constant, K, between RND and Hg(II), is determined from the slope to be 1.0×10^5 L mol^{-1}. The sensing behavior of RND toward Mg(II) was also studied, as shown in Fig. 8b.

It was of particular interest to investigate the reversibility of the system for the purpose of fabricating sensitive Hg(II) indicators. Upon addition of 4 equiv. of Na_2S to a solution mixture of 10 μmol L^{-1} RND and 40 μmol L^{-1} Hg(II), the color changed from pink to colorless. Additionally, the fluorescence intensity was quenched significantly, implying the decomplexation of Hg(II) by S^{2-} and a subsequent spirolactam ring closure reaction. Addition of another 40 μmol L^{-1} Hg(II) to this colorless solution produced an immediate color change back to pink, and the fluorescence intensity increased to approximately 95% of the original value. Subsequent additions of S^{2-} or Hg(II) revealed that this on/off cycle could be repeated at least three times, as shown in Fig. 9. Thus, RND can be classified as a reversible chemosensor for Hg(II).

Based on the thiophilic nature of Hg(II), it was reasonably assumed that the fluorescence intensity of RND–Hg(II) species would also be diminished upon addition of other sulfur-containing complexes. Both GSH and Cys are crucial thiol-containing biomolecules, and their detection is very important for investigat-

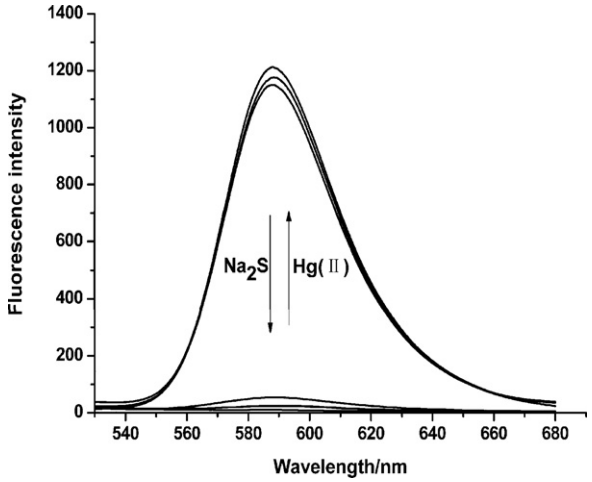

Fig. 9. Reversibility of 40 μmol L^{-1} Hg(II) coordinated to RND by Na_2S. The top set of lines represents the fluorescence enhancement that occurred after the addition of 40 μmol L^{-1} of Hg(II). The bottom set of lines represents emission from free RND (10 μmol L^{-1}) and the emission decrease that occurred after the addition of 40 μmol L^{-1} Na_2S to a solution containing [RND–Hg(II)] complex. Three on/off cycles by Hg(II)/Na_2S addition are depicted in this plot, with excitation at 500 nm.

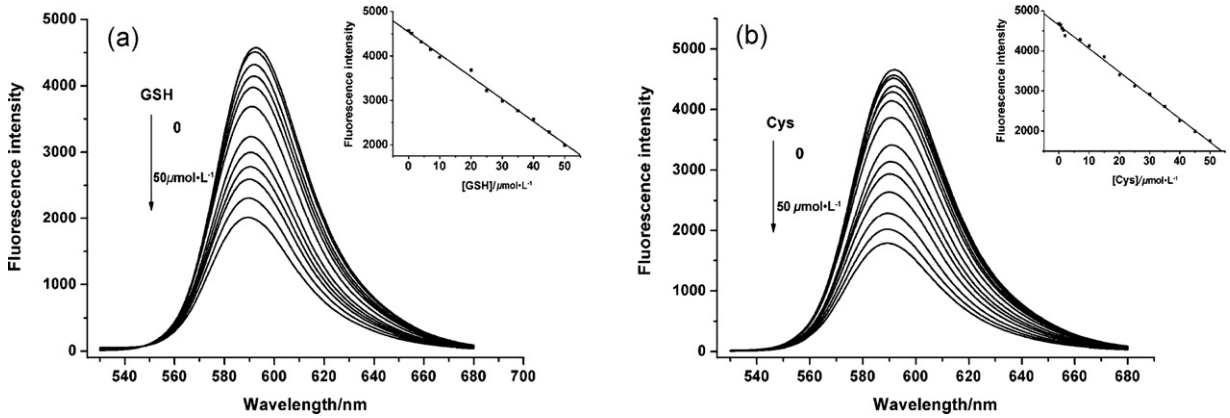

Fig. 10. (a) Changes in the fluorescence spectra of RND–Hg(II) measured in acetonitrile after the addition of different amounts of GSH (0–50 μmol L^{-1}). (b) Changes in the fluorescence spectra of RND–Hg(II) measured in acetonitrile after the addition of different amounts of Cys (0–50 μmol L^{-1}).

ing cellular function. Fig. 10 displays typical fluorescence spectra of the RND–Hg(II) complex system as functions of concentrations of added GSH and Cys from 5 to 50 μmol L^{-1}, respectively. In the absence of biothiols, RND fluorescence was relatively strong because of the spirolactam ring opening effect caused by Hg(II). In the presence of biothiols, however, the fluorescence of RND was quenched immediately because of the formation of the Hg(II)–S bond and subsequent RND ring-closure. From the insets of Fig. 10a and b, it can be observed that a good linear correlation (R = 0.997 for GSH and 0.998 for Cys) was obtained for both GSH and Cys. Therefore, biothiols were detected by RND indirectly.

We also proposed that RND would permeate into cells and be suited for fluorescence imaging of Hg(II) or Mg(II) in living cells because of its favorable amphiphilic and spectroscopic properties. Laser scanning confocal microscopy was used to investigate this proposition.

Cultured Hela cells were incubated with 100 μmol L^{-1} RND for 30 min at room temperature, and an insignificant amount of RND fluorescence was detected in the cells' interior (Fig. 11a). However, when the cells were supplemented with 100 μmol L^{-1} $Hg(NO_3)_2$ for another 30 min, a much brighter fluorescence from the intracellular area was observed (Fig. 11b). Bright field microscopic images (Fig. 11c) revealed that the cells were viable throughout the imaging experiments. An overlay of fluorescence and bright field images revealed that the fluorescence was localized in the perinuclear region of the cytosol (Fig. 11d), indicating the subcel-

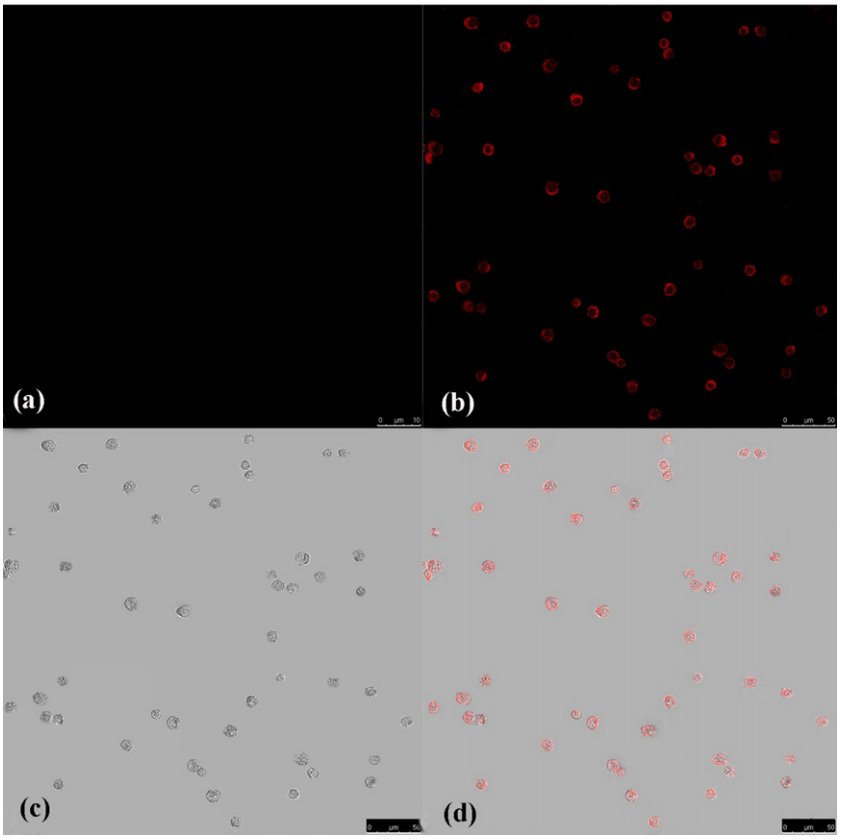

Fig. 11. (a) Fluorescence image of Hela cells incubated with 100 μmol L^{-1} RND for 30 min. (b) Confocal image of Hela cells that were further incubated with 100 μmol L^{-1} Hg(II) for another 30 min. (c) Bright field microscopic images of the cells shown in (b). (d) The overlaid image of (b) and (c). The excitation wavelength was 543 nm.

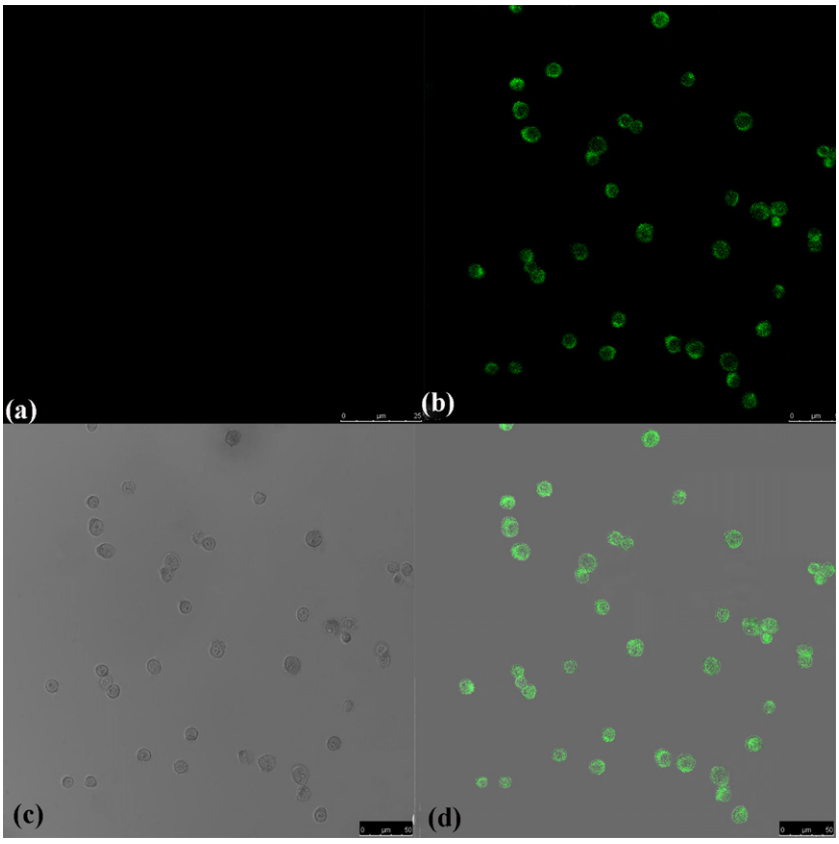

Fig. 12. (a) Fluorescence image of Hela cells incubated with 100 μmol L^{-1} RND for 30 min. (b) Confocal image of Hela cells that were further incubated with 100 μmol L^{-1} Mg(II) for another 30 min. (c) Bright field microscopic images of the cells shown in (b). (d) The overlaid image of (b) and (c). The excitation wavelength was 403 nm.

lular distribution of Hg(II). In a separate experiment, the cells were supplemented with 100 μmol L^{-1} Mg $(NO_3)_2$ instead of Hg $(NO_3)_2$, and the results are shown in Fig. 12. These results demonstrate that RND is cell permeable and capable of sensing both Hg(II) and Mg(II) in living cells.

4. Conclusions

In conclusion, we have synthesized a new rhodamine-based chemosensor that can achieve double-channel detection of Hg(II) and Mg(II) by different binding modes and can detect Hg(II) through visible color change. Selective binding of the compound to Hg(II) and Mg(II)caused immediate and remarkable fluorescence enhancement at different emission wavelengths, which proved that RND could serve as a sensitive and selective chemosensor of Hg(II) and Mg(II). Furthermore, we have demonstrated that RND is applicable for Hg(II) and Mg(II) imaging in living cells. In the presence of biothiols, such as GSH and Cys, fluorescence intensities were quenched linearly with increasing concentrations of such biothiols. As a result, these biothiols could be indirectly detected.

Acknowledgments

The work described in this paper was supported by the National Natural Science Foundation of China (Project No. 20803050) and the Specialized Research Fund for Instrument Program of the National Natural Science Foundation of China (20927007). We would like to express our sincere thanks to the Analytical & Testing Center of Sichuan University for the ^{1}H NMR measurements.

Appendix A. Supplementary data

Supplementary data associated with this article can be found, in the online version, at doi:10.1016/j.talanta.2011.07.070.

References

[1] W.F. Fitzgerald, C.H. Lamborg, C.R. Hammerschmidt, Chem. Rev. 107 (2007) 641–662.
[2] H.H. Harris, I. Pickering, G.N. George, Science 301 (2003) 1203.
[3] E.M. Nolan, S.J. Lippard, Chem. Rev. 108 (2008) 3443–3480.
[4] J.S. Kuwabara, Y. Arai, B.R. Topping, I.J. Pickering, G.N. George, Environ. Sci. Technol. 41 (2007) 2745–2749.
[5] C.Y. Li, X.B. Zhang, L. Qiao, Y. Zhao, C.M. He, S.Y. Huan, L.M. Lu, L.X. Jian, G.L. Shen, R.Q. Yu, Anal. Chem. 81 (2009) 9993–10001.
[6] L.Q. Guo, H. Hu, R.Q. Sun, G.N. Chen, Talanta 79 (2009) 775–779.
[7] J. Wang, B. Liu, Chem. Commun. 39 (2008) 4759–4761.
[8] H. Masuhara, H. Shioyama, T. Saito, K. Hamada, S. Yasoshima, N. Mataga, J. Phys. Chem. 88 (1984) 5868–5873.
[9] P. Svejda, A.H. Maki, R.R. Anderson, J. Am. Chem. Soc. 100 (1978) 7138–7145.
[10] B. Liu, Biosens. Bioelectron. 24 (2008) 756–760.
[11] Y.K. Che, X.M. Yang, L. Zang, Chem. Commun. 12 (2008) 1413–1415.
[12] Y. Yu, L.R. Lin, K.B. Yang, X. Zhong, R.B. Huang, L.S. Zheng, Talanta 69 (2006) 103–106.
[13] Y. Zhou, C.Y. Zhu, X.S. Gao, X.Y. You, C. Yao, Org. Lett. 12 (2010) 2566–2569.
[14] S. Voutsadaki, G.K. Tsikalas, E. Klontzas, G.E. Froudakis, H.E. Katerinopoulos, Chem. Commun. 46 (2010) 3292–3294.
[15] J.L. Fan, K.X. Guo, X.J. Peng, J.J. Du, J.Y. Wang, S.G. Sun, H.L. Li, Sens. Actuators B 142 (2009) 191–196.
[16] N.J. Birch (Ed.), Magnesium and the Cell, Academic Press Ltd., London, 1993.
[17] V. Trapani, G. Farruggia, C. Marraccini, S. Iotti, A. Cittadini, F.I. Wolf, Analyst 135 (2010) 1855–1866.
[18] F.I. Wolf, A. Torsello, S. Fasanella, A. Cittadini, Mol. Aspects Med. 24 (2003) 11–26.
[19] R.Y. Walder, B. Yang, J.B. Stokes, P.A. Kirby, X. Cao, P. Shi, C.C. Searby, R.F. Husted, V.C. Sheffield, Hum. Mol. Genet. 18 (2009) 4367–4375.
[20] M. Piskacek, L. Zotova, G. Zsurka, R.J. Schweyen, J. Cell. Mol. Med. 13 (2009) 693–700.

[21] W. Wang, L. Li, S.F. Liu, C.P. Ma, S.S. Zhang, J. Am. Chem. Soc. 130 (2008) 10846–10847.
[22] G.Y. Wu, Y.Z. Fang, S. Yang, J.R. Lupton, N.D. Turner, J. Nutr. 134 (2004) 489–492.
[23] J.R. Lakowicz, Principles of Fluorescence Spectroscopy, vol. 3, 3rd ed., Springer, NY, 2006, pp. 68–69.
[24] Q.J. Ma, X.B. Zhang, X.H. Zhao, Z. Jin, G.J. Mao, G.L. Shen, R.Q. Yu, Anal. Chim. Acta 663 (2010) 85–90.
[25] A. Chatterjee, M. Santra, N. Won, S. Kim, J.K. Kim, S.B. Kim, K.H. Ahn, J. Am. Chem. Soc. 131 (2009) 2040–2041.
[26] W. Huang, P. Zhou, W.B. Yan, C. He, L.Q. Xiong, F.Y. Li, C.Y. Duan, J. Environ. Monit. 11 (2009) 330–335.
[27] J.J. Du, J.L. Fan, X.J. Peng, P.P. Sun, J.Y. Wang, H.L. Li, S.G. Sun, Org. Lett. 12 (2010) 476–479.
[28] M. Suresh, S. Mishra, S.K. Mishra, E. Suresh, A.K. Mandal, A. Shrivastav, A. Das, Org. Lett. 11 (2009) 2740–2743.
[29] W. Jiang, W. Wang, Chem. Commun. 26 (2009) 3913–3915.
[30] K.C. Song, J.S. Kim, S.M. Park, K.C. Chung, S. Ahn, S.K. Chang, Org. Lett. 8 (2006) 3413–3416.
[31] S.K. Ko, Y.K. Yang, J. Tae, I. Shin, J. Am. Chem. Soc. 128 (2006) 14150–14155.
[32] K.W. Huang, H. Yang, Z.G. Zhou, M.X. Yu, F.Y. Li, X. Gao, T. Yi, C.H. Huang, Org. Lett. 10 (2008) 2557–2560.
[33] X.F. Yang, X.Q. Guo, Y.B. Zhao, Talanta 57 (2002) 883–890.
[34] F. Qian, C.L. Zhang, Y.M. Zhang, W.J. He, X. Gao, P. Hu, Z.J. Guo, J. Am. Chem. Soc. 131 (2009) 1460–1468.
[35] S.K. Kim, K.M.K. Swamy, S.Y. Chung, H.N. Kim, M.J. Kim, Y. Jeong, J. Yoon, Tetrahedron Lett. 51 (2010) 3286–3289.
[36] J.Y. Kwon, Y.J. Jang, Y.J. Lee, K.M. Kim, M.S. Seo, W. Nam, J. Yoon, J. Am. Chem. Soc. 127 (2005) 10107–10111.
[37] M. Suresh, A. Shrivastav, S. Mishra, E. Suresh, A. Das, Org. Lett. 10 (2008) 3013–3016.